

In-Field Comparison between G.652 and G.655 Optical Fibers for Polarization-Based Quantum Key Distribution

Costantino Agnesi,^{1,*} Massimo Giacomini,¹ Daniele Sartorato,^{1,2}
Silvia Artuso,² Giuseppe Vallone,¹ and Paolo Villoresi¹

¹*Dipartimento di Ingegneria dell'Informazione, Università degli Studi di Padova, Via Gradenigo 6B - 35131 Padua, Italy.*

²*Telebit S.p.A., Via Marco Fanno 1 - 31030 Casier (TV), Italy*

(Dated: December 8, 2023)

Integration of Quantum Key Distribution (QKD) in existing telecommunication infrastructure is crucial for the widespread adoption of this quantum technology, which offers the distillation of unconditionally secure keys between users. In this letter, we report a field trial between the *Points of Presence* (POPs) placed in Treviso and in Venezia - Mestre, Italy, exploiting the QuKy commercial polarization-based QKD platforms developed by ThinkQuantum srl and two different standards of single-mode optical fibers, i.e. *G.652* and *G.655*, as a quantum channel. In this field trial, several configurations were tested, including the co-existence of classical and quantum signals over the same fiber, providing a direct comparison between the performances of the G.652 and G.655 fiber standards for QKD applications.

I. INTRODUCTION

Quantum Key Distribution (QKD) is a quantum communication protocol that allows users to distill a secret key with unconditional security [1]. Differently from computationally-secure classical algorithms used in our current encryption systems, QKD offers long-term privacy guaranteed by the laws of Quantum Mechanics, and is not threatened by algorithmic and technological advances for both classical and quantum computation [2]. In fact, the strategic importance of QKD is highlighted by recent breakthroughs in quantum computing that accelerate the development of large-scale quantum computers capable of factorizing large prime numbers [3] that underlie our public cryptography schemes. Furthermore, QKD is the first quantum communication protocol to have reached industrialization and commercialization. This has led to several national and international initiatives that have incentivized the deployment of QKD systems in our telecommunications networks.

Two of the most commonly exploited optical fibers that are widely implemented in telecommunications are those described by the standards ITU-T G.652 [4] and ITU-T G.655 [5] enforced by the International Telecommunication Union. Both fiber types exhibit single-mode operations for both the 1310 nm and 1550 nm bands, and represent good choices for long-haul links. The dispersion properties of these two technologies are the aspect in which they differ the most. G.652 fibers are optimized for use in the 1310 nm band since they have zero dispersion at that wavelength. On the contrary, G.655 fibers are more suitable for the employment in the 1550 nm wavelength region due to their reduced dispersion value in the C-band (1530-1660 nm). G.655 fibers have a higher refractive index leading to a larger numerical aper-

ture and a wider acceptance angle, parameters that make these devices better suited for use in scenarios where it is challenging to control the launch conditions, such as in long distance or undersea communications. Furthermore, the G.655 show easy implementation with Erbium Doped Fiber Amplifiers (EDFA), making them appropriate for Wavelength Division Multiplexing (WDM) communication systems.



FIG. 1. Aerial view of the optical network exploited for the reported results. The two G.655 and G.652 optical fibers cover a link of about 19km between the cities of Treviso and Venice - Mestre, Italy. Map data: ©2022 Google.

To the best of our knowledge, a direct comparison between the performance of G.652 and G.655 fibers for QKD applications with polarization encoding has yet to be performed. This study, however, is of interest to the QKD community, as both standards are widely employed in telecommunications networks. In this letter, we report the results of a QKD field-trial exploiting both G.652 and

* costantino.agnesi@unipd.it

G.655 deployed between two urban centers in the Veneto region of Italy. The QKD system used in the trial was the QuKy systems of [ThinkQuantum srl](#), which implement the BB84 protocol [1] exploiting polarization encoding. By the QuKy system we performed a 24-hour trial for both the G.652 and the G.655 fiber channels in a “dark-fiber” configuration. Additionally, a co-existence test between quantum and classical signals was performed in both fibers.

II. METHODOLOGY

A. Optical network under test

The optical network considered in this study is represented by a deployed optical channel owned by the private telecom provider Retelit S.p.A. and operated by Telebit S.p.A., that connects the *Points of Presence* (POP) in the cities of Treviso and Venezia - Mestre for a distance of approximately 19 km, as it can be observed in Fig. 1. The two optical fibers are installed in parallel, and for this reason are considered to be exposed to the same macroscopic mechanical and thermal stresses. This configuration is optimal for this study, as it allows for a parallel comparison between the two systems, including channel perturbations due to the external environment. Lastly, these fibers are buried underground, making them less affected by optical and mechanical disturbances. From a usage point of view, the G.655 fiber used in the study is part of a 36 fiber bundle, composed of 3 micro-tubes with 94% occupation of active data transmission. Instead, the G.652 fiber used in the study is part of a 72 fiber bundle, composed of 6 micro-tubes, with a much lower occupation rate of only 8%.

	Fiber	
	G.652	G.655
α [dB/km] @ 1310 nm	0.3251 ± 0.0001	0.3814 ± 0.0001
α [dB/km] @ 1550 nm	0.1862 ± 0.0001	0.2383 ± 0.0001
α^{tot} [dB] @ 1310 nm	6.0764 ± 0.0005	6.9420 ± 0.0005
α^{tot} [dB] @ 1550 nm	3.4810 ± 0.0005	4.3380 ± 0.0005
Total Length [km]	18.692 ± 0.001	18.201 ± 0.001

TABLE I. Results of the OTDR analysis for both fibers.

A preliminary characterization of the two optical fibers considered in this study was performed in order to foresee their performances in classical and quantum communications. For this, an optical-time domain reflectometer (OTDR) test was firstly conducted, providing the results reported in Tab. I. As expected, both fibers manifest a lower attenuation coefficient α for 1550 nm wavelength, with respect to the 1310 nm. Furthermore, according to the inferred results the standard G.652 offers less atten-

uation with respect to its counterpart, regardless of the considered wavelength. The slight length differences observed in the two fibers can be explained by the diversity between the end reels placed at the end of each link during the OTDR analysis.

The second phase of the characterization of the optical network consisted in performing a *Polarization Drift Measurement*, which allows to understand the stability of the specific considered optical fiber as a quantum channel in the implementation of a QKD protocol. As a matter of fact, quantum cryptographic techniques based on polarization states as encoding strategy require some polarization stability in order to retrieve the information shared among the users legitimately connected to the network. However, if the drift is slow enough, it is possible to characterize the rotation of polarization introduced by the birefringence of the fiber and restore the initial information sent through it using polarization controllers. Polarization drift characterization was performed by injecting 1550 nm polarized light into both fibers and measuring the polarization state after the fiber propagation using a polarimeter. We estimated a drift of around 23 mrad/s for both G.652 and G.655 fibers. This value was calculated as the scalar product computation between the subsequent samples obtained every second. The inferred result is well compatible with the polarization tracking capabilities of polarization-based QKD receivers [6].

Furthermore, with these measurements we verified the robustness against polarization fluctuation of the G.652 and G.655, showing long-term stability without significant polarization rotation of the transmitted quantum states, as can be proven by 2.

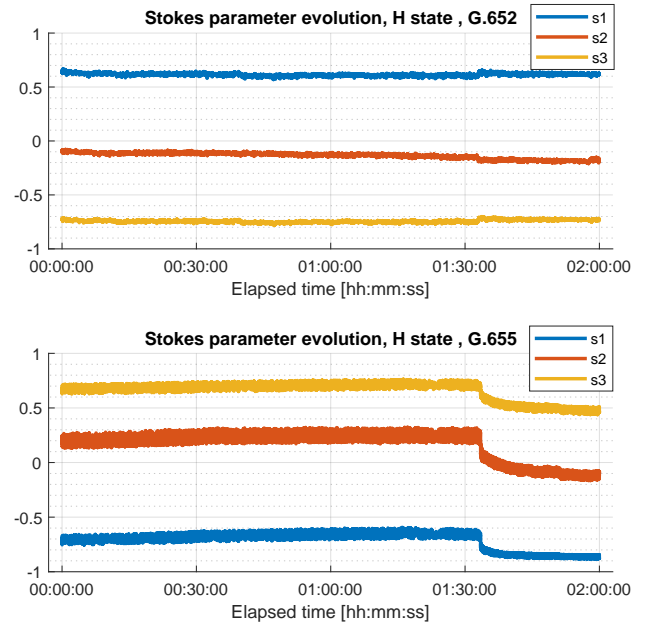


FIG. 2. Evolution of the Stokes parameters in time for the two considered fiber standards.

B. Quantum Key Distribution system

The QKD device used in this field trial was the QuKy system developed by ThinkQuantum srl, which implements the BB84 protocol encoded with three states and one decoy polarization [7]. This simplified protocol has the same level of security and performance as the original BB84 protocol [8], whereas the one-decoy scheme can provide higher rates in the finite-key scenario compared to the two-decoy scheme [9]. The transmission of quantum signals is performed at 1550 nm, ensuring full compatibility with standard fiber-optic networks and components. The QuKy transmitter offers stable, low-error, and calibration-free polarization encoding by using the iPOGNAC modulator, which is described in Ref. [10]. Furthermore, in contrast to proof-of-concept QKD demonstrations [11], the QuKy devices perform “real QKD” since phase randomization is performed via laser gain switching [12] and the randomness is provided by a source-device-independent Quantum Random Number Generator [13] integrated inside the QKD transmitter (QRN2Qubit direct stream).

The quantum receiver decodes the quantum signals exploiting a polarimetric scheme that implements state projection into two mutually unbiased bases, whereas single-photon detection is performed using InGaAs/InP single-photon avalanche detectors (SPAD). Since both transmitter and receiver are fully contained in a 2U 19” Rack-mount enclosure, the system can be easily integrated in telecom data centers, such as the Treviso and Venezia - Mestre POPs. To compensate for the random and dynamic unitary transformation induced by the fiber-optical channel, the QuKy receiver integrates an all-fiber polarization controller. The correction signal applied to this polarization controller is given by a set of publicly disclosed qubits interleaved with the random qubit transmission. This allows for a quick determination of QBER and a rapid feedback cycle [14], without requiring a dedicated feedback system composed of separate lasers and detectors. Furthermore, temporal synchronization is performed via the Qubits4Sync algorithm [15] to synchronize the frequency and absolute time between the transmitter and receiver device. This implies that the QuKy system does not require any synchronization subsystem, which is usually implemented with a pulsed laser or GNSS clock to share an external time reference.

C. Field-trials configurations

The fibers were tested in two configurations, labeled as *dark-fiber* and *CQ-coexistence*.

1. Dark-Fiber

This configuration represents an implementation of the QKD protocol in which the quantum channel and the classical channel are separated and realized with two different optical fibers. In this configuration, the classical signals were encoded at 1490 nm using bidirectional SFP transceivers, while the quantum signals were emitted at 1550 nm, as described in the previous section.

2. CQ-coexistence

In our QKD field-trial, the *coexistence* configuration refers to the simultaneous operation of classical and quantum communications in the same fiber via wavelength division multiplexing (WDM). This scheme is of particular interest for the widespread adoption of QKD in telecommunication networks, since the integration of QKD with other communication systems can lead to a reduction in the high costs of the deployment and maintenance of quantum optical networks [16].

The setup used to implement the coexistence of QKD with classical communication is depicted in Fig. 3. Classic communication was carried out using duplex SFP transceivers working at 1310 nm. This wavelength was chosen to have sufficient spectral separation between the classical and quantum signals and to enable the use of commercial off-the-shelf WDM filters. In particular, coarse WDMs were used to merge and separate the 1310 nm light from the 1550 nm quantum signal, and a more dense WDM allowed for narrow (0.8 nm) filtering at the QKD wavelength (C34 according to the ITU G.694.1 spectral grid). Additionally, the duplex configuration of the SFP transceivers allowed us to test two different possible implementations. The first one was the co-propagation scheme where the quantum signals propagated together with the classical signal sent from Alice to Bob, while the classical signals sent from Bob to Alice exploited a separate optical fiber. The second implementation was the counterpropagation scheme, where the quantum signals, still sent from Alice to Bob, propagated in the same channel but in opposite direction of the classical signal sent from Bob to Alice, while the classical signals sent from Alice to Bob exploited a separate optical fiber.

In order to reduce the interference between the quantum and classical signals, a Variable Optical Attenuator (VOA) was inserted after the SFP responsible for emitting the light co-propagating with the QKD signal. This VOA was set at the maximum attenuation possible that still guaranteed the nominal 10 Gbps connection, which led to a launch power of the classical signal of approximately -24 dBm in the case of the G.652 fiber and about -23 dBm for the G.655 fiber.

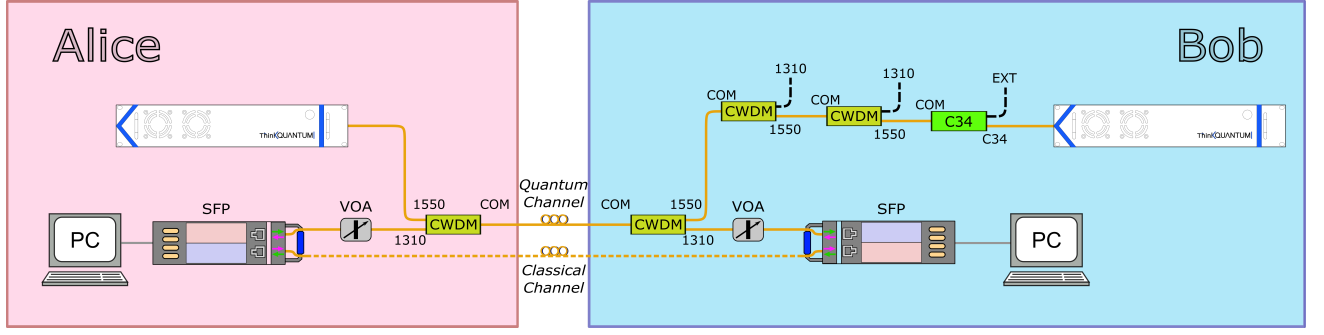


FIG. 3. Graphical representation of the experimental setup required to analyze the optical fibers in Coexistence Duplex configuration. VOA: Variable Optical Attenuator, CWDM: Coarse Wavelength Division Multiplexer, C34: optical filter. The green arrows in the SFP ports indicates the direction of the optical signal in the *co-propagation* configuration, while the pink arrows represent the *counter-propagation* configuration.

III. RESULTS

A. QKD 24-hour test in dark fiber configuration

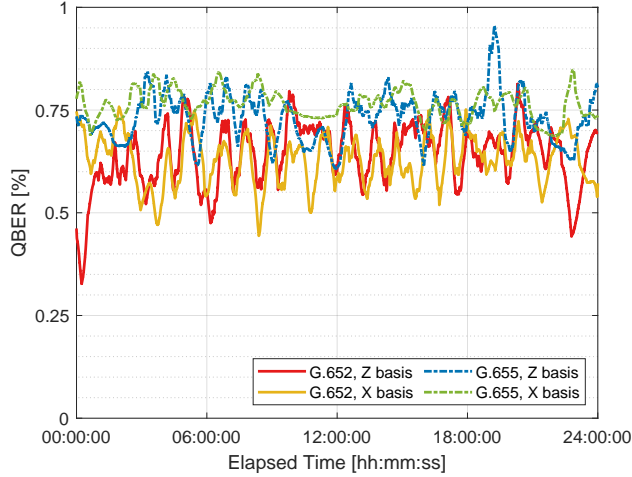


FIG. 4. 24 hours time evolution of the QBER considering the two key (\mathcal{Z}) and *control* (\mathcal{X}) bases together with their lowerbounds.

Between Wednesday, November 30th 2022, and Thursday, December the 1st 2022, we performed the first QKD test exploiting the G.652 as quantum channel, beginning at 12 : 00 am (CET) and lasting for exactly 24 hours. Subsequently, at 01 : 00 pm (CET) of Thursday, December the 1st, the test on the G.655 fiber started, lasting until 01 : 00 pm (CET) of Friday, December the 2nd. The days of the test can be considered typical weekdays, all of which exhibit temperate winter weather with a daily average temperature of 7°.

To assess the performance of the QKD system, we monitored the main key performance indicators, i.e., *Quantum Bit Error Rate* (QBER), *Sifted Key Rate* and

Secure Key Rate (SKR). The results on QBER are shown in Fig. 4, while the Sifted Key Rate and SKR are shown in Fig. 5, computed considering the finite-key effects with security parameter $\epsilon_{\text{sec}} = 10^{-15}$.

Regarding the G.652 fiber we report an average QBER of $(0.64 \pm 0.30)\%$ in the key-generating \mathcal{Z} basis and $(0.65 \pm 0.48)\%$ in the control state of the \mathcal{X} basis. An average of 14264 ± 1260 of bits were sifted per second, resulting in an average secret key generation of 4460 ± 357 bits per second and a total generation of 392 megabits of secret key material. Instead, for the G.655 fiber, we report an average QBER of $(0.73 \pm 0.31)\%$ in the key-generating \mathcal{Z} basis and $(0.78 \pm 0.19)\%$ in the control state. An average of 12736 ± 1015 bits per second were sifted resulting in an average secret key generation of 2869 ± 236 bits per second and a total generation of 296 megabits of secret key material.

Small fluctuations in the QBER are interpreted as an expected effect of the birefringence of the optical fibers, which may be affected by predictable environmental stresses. These determine mild oscillations in the final Sifted and Secret Key Rates. However, the resulting QBER shows the robustness and suitability of the fibers under test, remaining below the threshold of 1%

B. Co-existence Results

On the afternoon of December, the 2nd, after the completion of the 24 hour run in the G655 fiber, we performed a series of experiments to test the co-existence of QKD with classical communication on the same fiber. As thoroughly explained in Sect. II C 2, these included co-propagation and counter-propagation of a 1310 nm classical signal together with the 1550 nm QKD signal. The results of the coexistence experiment are reported in Tab. II where the most significant parameters as the QBERs, the SNR, the Sifted Key Rate and the Secret Key Rate are shown for the two optical fibers under test. As before, the SKR was calculated using the finite-key approach.

<i>Configuration</i>	Co-P. G.652	Counter-P. G.652	Co-P. G.655	Counter-P. G.655
QBER Z [%]	1.7 ± 1.4	1.4 ± 0.4	2.9 ± 0.7	2.5 ± 0.5
QBER X [%]	1.9 ± 0.8	2.0 ± 0.3	3.7 ± 1.1	3.1 ± 0.3
SNR	40.2 ± 2.4	37.2 ± 2.2	17.9 ± 1.2	20.2 ± 1.1
Noise [events/s]	7600 ± 600	8200 ± 400	12000 ± 1700	11000 ± 500
Sifted KR [kb/s]	10.8 ± 1.1	10.7 ± 1.0	7.8 ± 0.4	7.9 ± 0.4
Secure KR [b/s]	2400 ± 300	2000 ± 600	21 ± 15	48 ± 62

TABLE II. Results of the coexistence test for both the co-propagation (*Co-P.*) and counter-propagation (*Counter-P.*) configurations, studied considering the two optical fibers under test, i.e. G.652 and G.655.

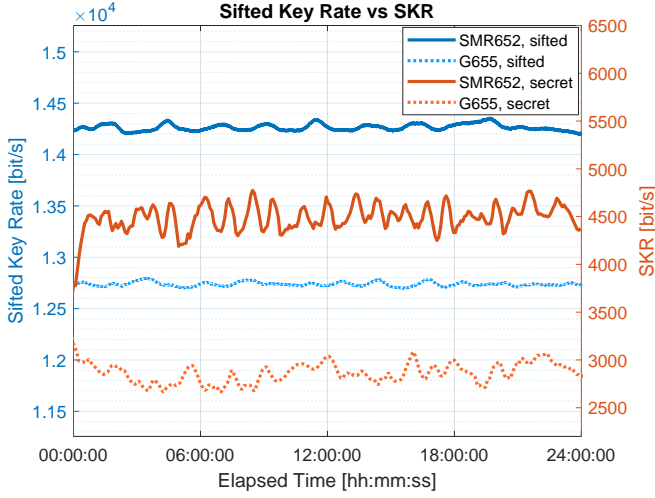


FIG. 5. Time evolution of the *Key Rates*: *Sifted* in *blue* on the left axis and *Secret* in *orange* on the right axis.

IV. DISCUSSION

The Sifted and Secret Key Rate results reported for the dark fiber configuration are in line with expectations since the performance distinctions can be mainly explained by the difference in the total losses for both fiber standards. However, more considerations must be made to interpret the lower QBER observed in the G.652 fiber channel, which is due to a higher Signal-to-Noise Ratio (SNR) of 208.44 ± 22.62 compared to 105.19 ± 8.79 of the G.655 fiber. In fact, this last result is partially unexpected if just a total loss dependence on the SNR is taken into account. Indeed, the halving of the final SNR moving from G.652 to G.655 suggests further causes in addition to the 1 dB signal losses introduced by the NZD standard. An explanation could be based on the much higher occupation rate of the G.655 fiber bundle used in the experiment, which could have introduced crosstalk between adjacent fibers, as suggested by the increase of the observed noise level. However, we would

like to stress that the overall QKD performance in both fiber standards can be thought to be excellent, especially when considering that they were obtained from deployed fibers used for day-to-day telecommunications between the Venezia - Mestre and Treviso POPs.

The co-existence configurations showed a relevant distinction in performance between the G.652 and the G.655 standards. Whereas secure key generation was possible in all tested configurations for both fiber standards, the SKR obtained with the G.652 fiber was around two orders of magnitude higher than with G.655 standard. This difference in SKR can be attributed to a higher QBER observed in the G.655, also reflected in a higher SNR for the G.652 fiber. This difference in SNR is only partially explained by the lower signal rate observed in the G.655 due to its higher attenuation. Higher noise levels were also observed in the G.655 channel, mainly due to a higher stimulated Raman scattering [17] caused by the higher launch power of the classical channel.

V. CONCLUSIONS

In summary, we have assessed the performances of deployed G.652 and G.655 fibers used as quantum channel for a QKD protocol based on polarization encoding implemented by ThinkQuantum's QuKy platform. This study constitutes a first attempt to classify and characterize different standards in optical fibers for quantum communications, hence further theoretical and experimental studies must be performed to understand the difference in terms of noise and transmissivity when alternative physical links are implemented.

Furthermore, additional optimizations should be performed for the coexistence trial, especially when exploiting the more lossy G.655 standard. As a matter of fact, in the case of exploiting more than one wavelength, several non-linear phenomena may occur, such as Raman Scattering or Four-Wave Mixing, that collectively contribute to increase the noise at the detection side.

Lastly, this work represents a concrete example of a fully functioning commercial QKD system being integrated in a deployed and operating network, demonstrat-

ing that QKD technology can be exploited in real-case scenarios.

ACKNOWLEDGMENTS

We would like to thank [Telebit S.p.A.](#) for technical support and general assistance in the measurement campaign, with a particular effort for the OTDR metering, as well as [Retelit S.p.A.](#) for having provided the characterized optical network.

Funding: PhD scholarship of MG was co-funded by [Telebit S.p.A.](#) and MIUR - Ministerial Decree 352/2022. This work was partially funded by the European Union (QUID project, GA 101091408). Views and opinions expressed are however those of the author(s) only and do not necessarily reflect those of the European Union or the European Commission-EU. Neither the European Union nor the granting authority can be held responsible for them.

-
- [1] C. H. Bennett and G. Brassard, Quantum cryptography: Public key distribution and coin tossing, [Theor. Comput. Sci.](#) **560**, 7 (2014).
 - [2] S. Pirandola, U. L. Andersen, L. Banchi, M. Berta, D. Bunandar, R. Colbeck, D. Englund, T. Gehring, C. Lupo, C. Ottaviani, J. L. Pereira, M. Razavi, J. Shamsul Shaari, M. Tomamichel, V. C. Usenko, G. Vallone, P. Villoresi, and P. Wallden, Advances in quantum cryptography, [Adv. Opt. Photonics](#) **12**, 1012 (2020).
 - [3] P. Shor, Polynomial-time algorithms for prime factorization and discrete logarithms on a quantum computer, [SIAM J. Comput.](#) **26**, 1484 (1997).
 - [4] Rec. ITU-T G.652, [Characteristics of a single-mode optical fibre and cable](#) (2016).
 - [5] Rec. ITU-T G.655, [Characteristics of a non-zero dispersion-shifted single-mode optical fibre and cable](#) (2009).
 - [6] Y.-Y. Ding, H. Chen, S. Wang, D.-Y. He, Z.-Q. Yin, W. Chen, Z. Zhou, G.-C. Guo, and Z.-F. Han, Polarization variations in installed fibers and their influence on quantum key distribution systems, [Opt. Express](#) **25**, 27923 (2017).
 - [7] F. Grünenfelder, A. Boaron, D. Rusca, A. Martin, and H. Zbinden, Simple and high-speed polarization-based QKD, [Appl. Phys. Lett.](#) **112**, 051108 (2018).
 - [8] K. Tamaki, M. Curty, G. Kato, H.-K. Lo, and K. Azuma, Loss-tolerant quantum cryptography with imperfect sources, [Phys. Rev. A](#) **90**, 052314 (2014).
 - [9] D. Rusca, A. Boaron, F. Grünenfelder, A. Martin, and H. Zbinden, Finite-key analysis for the 1-decoy state QKD protocol, [Appl. Phys. Lett.](#) **112**, 171104 (2018).
 - [10] M. Avesani, C. Agnesi, A. Stanco, G. Vallone, and P. Villoresi, Stable, low-error, and calibration-free polarization encoder for free-space quantum communication, [Opt. Lett.](#) **45**, 4706 (2020).
 - [11] D. Ribezzo, M. Zahidy, I. Vagniluca, N. Biagi, S. Francesconi, T. Occhipinti, L. K. Oxenløwe, M. Lončarić, I. Cvitić, M. Stipčević, v. Pušavec, R. Kaltenbaek, A. Ramšak, F. Cesa, G. Giorgetti, F. Scazza, A. Bassi, P. De Natale, F. S. Cataliotti, M. Inguscio, D. Bacco, and A. Zavatta, Deploying an inter-european quantum network, [Adv. Quantum Technol.](#) **6**, 2200061.
 - [12] T. Kobayashi, A. Tomita, and A. Okamoto, Evaluation of the phase randomness of a light source in quantum-key-distribution systems with an attenuated laser, [Phys. Rev. A](#) **90**, 032320 (2014).
 - [13] M. Avesani, D. G. Marangon, G. Vallone, and P. Villoresi, Source-device-independent heterodyne-based quantum random number generator at 17 Gbps, [Nat. Commun.](#) **9**, 5365 (2018).
 - [14] C. Agnesi, M. Avesani, L. Calderaro, A. Stanco, G. Folletto, M. Zahidy, A. Scriminich, F. Vedovato, G. Vallone, and P. Villoresi, Simple quantum key distribution with qubit-based synchronization and a self-compensating polarization encoder, [Optica](#) **7**, 284 (2020).
 - [15] L. Calderaro, A. Stanco, C. Agnesi, M. Avesani, D. Dequal, P. Villoresi, and G. Vallone, Fast and simple qubit-based synchronization for quantum key distribution, [Phys. Rev. Appl.](#) **13**, 054041 (2020).
 - [16] P. D. Townsend, Simultaneous quantum cryptographic key distribution and conventional data transmission over installed fibre using wavelength-division multiplexing, [Electron. Lett.](#) **33**, 188 (1997).
 - [17] M. F. S. Ferreira, Stimulated raman scattering, in [Nonlinear Effects in Optical Fibers](#) (John Wiley & Sons, Ltd, 2011) Chap. 11, pp. 245–272.